

# Determination of Basicity of Core X and Terminal Y Ligands (X, Y = S and Se) of Reduced, Oxidized, and Super-Oxidized Forms of $[\text{Fe}_4\text{X}_4(\text{YAd})_4]^{2-}$ (Ad = 1-Adamantyl) in Aqueous Solutions

Masami Nakamoto,\* Kenji Fukaishi, Tsuyoshi Tagata, Hide Kambayashi,† and Koji Tanaka\*†

Osaka Municipal Technical Research Institute, Morinomiya, Joto-ku, Osaka 536-8553

†Institute for Molecular Science, Myodaiji, Okazaki 444-8585

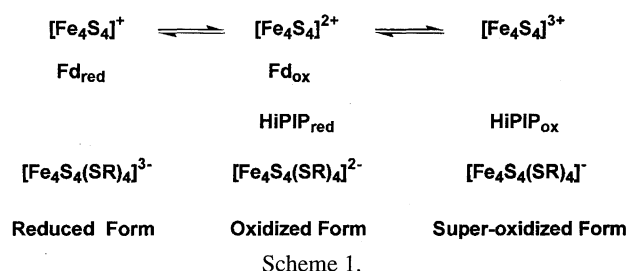
(Received August 5, 1998)

A series of  $[\text{Fe}_4\text{X}_4(\text{YAd})_4]^{2-}$  (X, Y = S, Se; Ad = 1-adamantyl) were prepared as a model of high potential iron–sulfur proteins. Hydrolysis of the clusters was effectively depressed in aqueous poly[2-(dimethylamino)hexanamide] (PDAH) solutions due to the embedding effect in hydrophobic environment and/or inhibition of dissociation of the terminal ligand into the aqueous media. Cyclic voltammetry of those clusters in aqueous PDAH solutions showed pH-dependent redox potentials of not only the  $[\text{Fe}_4\text{X}_4]^{+/2+}$  but also the  $[\text{Fe}_4\text{X}_4]^{2+/3+}$  (X = S and Se) couples, resulting from redox-linked protonation reactions of three oxidation states of  $[\text{Fe}_4\text{X}_4(\text{YAd})_4]^{n-}$  ( $n = 1-3$ ).  $\text{p}K_a$  values of the reduced, oxidized, and super-oxidized forms of  $[\text{Fe}_4\text{X}_4(\text{YAd})_4]^{2-}$  were determined by computer simulation of the pH dependent redox potentials. The basicity of the core X (X = S and Se) of three oxidation states of  $[\text{Fe}_4\text{X}_4(\text{YAd})_4]^{n-}$  ( $n = 1, 2, 3$ ) was stronger than the terminal YAd (Y = S and Se) ligands: in the case of the mono-protonated  $[\text{Fe}_4\text{X}_4(\text{YAd})_4]^{3-}(\text{H}^+)$  and  $[\text{Fe}_4\text{X}_4(\text{YAd})_4]^{2-}(\text{H}^+)$ , basicity of the terminal YAd ligand of  $[\text{Fe}_4\text{X}_4(\text{YAd})_4]^{2-}(\text{H}^+)$  becomes stronger than that of core X, although the core X of  $[\text{Fe}_4\text{X}_4(\text{YAd})_4]^{3-}(\text{H}^+)$  still showed a stronger basicity than those of terminal YAd ligands.

Iron–sulfur proteins play key roles as electron transfer catalysts in various biological redox reactions such as photosynthesis,<sup>1)</sup> nitrate reduction,<sup>2)</sup> and dinitrogen fixation.<sup>3)</sup> There are two types of iron–sulfur proteins that have  $\text{Fe}_4\text{S}_4$  redox active centers; one is 4Fe ferredoxins (Fd),<sup>4)</sup> and the other is high-potential iron–sulfur proteins (HiPIP).<sup>5)</sup> The redox potentials of these iron–sulfur proteins differ by about 1 V,<sup>6)</sup> deriving from different redox couples: 4Fe Fds mediate electron transfer reactions through the  $[\text{Fe}_4\text{S}_4]^{+/2+}$  redox couple in the range of  $E_{1/2} = -0.52$  to  $-0.73$  V (vs. SCE),<sup>4–6)</sup> and HiPIPs act as electron transfer catalysts through the  $[\text{Fe}_4\text{S}_4]^{2+/3+}$  redox couple<sup>7)</sup> with  $E_{1/2}$  values around 0 V (vs. SCE) in  $\text{H}_2\text{O}$  at pH 7,<sup>8)</sup> as shown in Scheme 1. Structural studies on HiPIPs show that the metal center is decidedly located in hydrophobic spheres including NH–S hydrogen bonds between the sulfur atoms of the  $\text{Fe}_4\text{S}_4$  core and/or the sulfur atoms of the terminal cysteine residue and peptide NH–protons.<sup>9,10)</sup> The specific redox potential of the HiPIPs ( $E_{1/2} = \text{ca. } 0$  V vs. SCE)<sup>8)</sup> would be largely influ-

enced by such hydrogen bonds<sup>11)</sup> caused by peptide chains.

Synthetic  $\text{Fe}_4\text{S}_4$  clusters with alkane- and arenethiolate ligands and  $[\text{Fe}_4\text{S}_4(\text{SR})_4]^{2-}$  as models of 4Fe Fds have been extensively studied and well simulate the  $[\text{Fe}_4\text{S}_4]^{+/2+}$  redox reactions in organic solvents.<sup>12)</sup> Most of the  $[\text{Fe}_4\text{S}_4(\text{SR})_4]^{2-}$  clusters, however, are subject to decomposition upon one-electron oxidation in DMF,  $\text{CH}_3\text{CN}$ , and DMSO,<sup>13)</sup> in contrast to HiPIPs. Stable  $[\text{Fe}_4\text{S}_4]^{2+/3+}$  redox couples in dry organic solvents are observed only in 2,4,6-tri(isopropyl)benzenethiolate,<sup>14)</sup> polypeptide,<sup>15)</sup> and the 36-membered ring<sup>16)</sup> ligated  $\text{Fe}_4\text{S}_4$  clusters, and so the stabilization of the super-oxidized form  $[\text{Fe}_4\text{S}_4(\text{SR})_4]^-$  has been attributed to inhibition of solvent attack on the  $[\text{Fe}_4\text{S}_4]^{3+}$  core by those sterically encumbered thiolate ligands. Coordination geometry of the metal center is also important in conformation control for model peptides with the Cys–X–Y–Cys amino acid sequence, with NH–S hydrogen bonds.<sup>17)</sup> Ueyama and Nakamura have demonstrated that intra-molecular NH–S hydrogen bond formation in the  $\text{Fe}_4\text{S}_4$  model clusters causes large positive shifts of the redox potentials in  $\text{CH}_3\text{CN}$ .<sup>18)</sup> A similar positive shift of the redox potentials by NH–S hydrogen bonds is also observed in other model complexes for rubredoxins,<sup>19)</sup> cytochrome P-450,<sup>20)</sup> molybdoenzymes,<sup>21)</sup> and blue copper proteins.<sup>22)</sup> The existence of stable NH–S hydrogen bondings in 4Fe–4S proteins reflects the basicity of core and terminal sulfur ligands. Measurement of the basicity of the sulfur ligands of synthetic  $\text{Fe}_4\text{S}_4$  clusters in the three oxidation states (Scheme 1) must serve for the understanding the electronic structures of Fds and HiPIPs. Accordingly, a com-



parative study on the redox behavior of synthetic  $\text{Fe}_4\text{S}_4$  and  $\text{Fe}_4\text{Se}_4$  clusters under aqueous conditions is well suited for the measurement of the basicity of sulfur ligands, if hydrolysis of  $\text{Fe}_4\text{X}_4$  ( $\text{X} = \text{S}$  and  $\text{Se}$ ) clusters can be depressed under aqueous conditions. Along this line, we have demonstrated that  $[\text{Fe}_4\text{S}_4(\text{SAd})_4]^{2-}$  ( $\text{Ad} = 1\text{-adamantyl}$ ) solubilized in aqueous poly[2-(dimethylamino)hexanamide] (PDAH) solutions (PDAH:  $[-\text{NHCH}_2\text{CH}_2\text{CH}_2\text{CH}_2\text{C}(\text{NMe}_2)\text{HCO-}]_n$ ) shows that stable  $[\text{Fe}_4\text{S}_4]^{+/2+}$  and  $[\text{Fe}_4\text{S}_4]^{2+/3+}$  redox couples accompanied protonation of  $[\text{Fe}_4\text{S}_4]^{n+}$  ( $n = 1-3$ ).<sup>23,24</sup> In this paper we report the evaluation of the basicity of core S and terminal S ligands of the  $\text{Fe}_4\text{S}_4$  clusters on the basis of the redox-linked protonation behavior of  $[\text{Et}_4\text{N}]_2[\text{Fe}_4\text{X}_4(\text{YAd})_4]$  ( $\text{X}, \text{Y} = \text{S}$  and  $\text{Se}$ ;  $\text{Ad} = 1\text{-adamantyl}$ ) in aqueous PDAH solutions.

## Experimental

**General Procedure and Materials.** All manipulations in the preparation of compounds and their physical measurements were performed under an  $\text{N}_2$  atmosphere. Solvents used for preparation and physical measurements were distilled over dehydration chemicals: sodium methoxide for MeOH, sodium for diethyl ether, and calcium oxide for DMF. Commercially available 1-bromoadamantane (AdBr) was purified by recrystallization from MeOH. Selenourea supplied by Shinko Chemical Co., Ltd. was used without purification. 1-Adamantanethiol AdSH and -selenol AdSeH were prepared by the reaction of AdBr with thiourea and selenourea, respectively, by the methods in the literatures.<sup>25,26</sup>  $[\text{Et}_4\text{N}]_2[\text{Fe}_4\text{S}_4(\text{S}-t\text{-Bu})_4]$ ,<sup>27</sup>  $[\text{Et}_4\text{N}]_2[\text{Fe}_4\text{Se}_4(\text{S}-t\text{-Bu})_4]$ ,<sup>28</sup> and  $[\text{Et}_4\text{N}]_2[\text{Fe}_4\text{S}_4(\text{SAd})_4]^{2-}$ <sup>23</sup> were prepared as described in the literature. Poly[2-(dimethylamino)hexanamide] (PDAH) supplied by Toray Co., Ltd. was purified by dialysis.

**Preparation of  $[\text{Et}_4\text{N}]_2[\text{Fe}_4\text{S}_4(\text{SeAd})_4]$ .** The selenolate ligated cluster  $[\text{Et}_4\text{N}]_2[\text{Fe}_4\text{S}_4(\text{SeAd})_4]$  was prepared by the ligand substitution reaction<sup>29</sup> of  $[\text{Fe}_4\text{S}_4(\text{S}-t\text{-Bu})_4]^{2-}$  with AdSeH as follows; a DMF (60  $\text{cm}^3$ ) solution containing  $[\text{Et}_4\text{N}]_2[\text{Fe}_4\text{S}_4(\text{S}-t\text{-Bu})_4]$  (0.51 g, 0.53 mmol) and AdSeH (1.36 g, 6.32 mmol) was stirred at 55 °C for 10 h, during which time  $\text{N}_2$  gas was bubbled into the solution every 15 min to remove  $t\text{-BuSH}$  from the solution. The resulting solution was evaporated to dryness under reduced pressure. The residual solid was washed by diethyl ether (50  $\text{cm}^3 \times 3$ ), collected by filtration, dried in vacuo, 97% yield. Found: C, 45.63; H, 6.80; N, 2.39%. Calcd for  $\text{C}_{56}\text{H}_{100}\text{Fe}_4\text{N}_2\text{S}_4\text{Se}_4$ : C, 45.79; H, 6.86; N, 1.91%.

**Preparation of  $[\text{Et}_4\text{N}]_2[\text{Fe}_4\text{Se}_4(\text{SAd})_4]$ .** To a MeOH (40  $\text{cm}^3$ ) solution containing MeOLi (1.64 g, 43.2 mmol) and AdSH (7.11 g, 42.3 mmol) was added a filtered solution of  $\text{FeCl}_3$  (1.71 g, 10.6 mmol), followed by the addition of selenium powder (0.84 g, 10.6 mmol). After this was stirred for 20 h at room temperature, the resulting solution was filtered. To the filtrate  $\text{Et}_4\text{NBr}$  (1.68 g, 8.0 mmol) in MeOH (20  $\text{cm}^3$ ) was added slowly to give black crystals, which were collected by filtration, washed with a small amount of MeOH, and dried in vacuo, with 64.7% yield. Found: C, 45.75; H, 6.79; N, 1.84%. Calcd for  $\text{C}_{56}\text{H}_{100}\text{Fe}_4\text{N}_2\text{S}_4\text{Se}_4$ : C, 45.79; H, 6.86; N, 1.91%.

**Preparation of  $[\text{Et}_4\text{N}]_2[\text{Fe}_4\text{Se}_4(\text{SeAd})_4]$ .** A DMF (60  $\text{cm}^3$ ) solution containing  $[\text{Et}_4\text{N}]_2[\text{Fe}_4\text{S}_4(\text{S}-t\text{-Bu})_4]$  (0.48 g, 0.41 mmol) and AdSeH (1.05 g, 4.88 mmol) was stirred at 55 °C for 10 h, during which time  $\text{N}_2$  gas was bubbled into the solution. The resulting solution was evaporated to dryness under reduced pressure. The

residual solid was washed with diethyl ether (50  $\text{cm}^3$ ), collected by filtration, dried in vacuo, with 95% yield. Found: C, 40.28; H, 6.15; N, 2.18%. Calcd for  $\text{C}_{56}\text{H}_{100}\text{Fe}_4\text{N}_2\text{Se}_8$ : C, 40.60; H, 6.08; N, 1.69%.

**Preparation of Aqueous PDAH Solutions.** A DMF (1.0  $\text{cm}^3$ ) solution of the cluster (20  $\mu\text{mol}$ ) was added to a stirred aqueous solution (12  $\text{cm}^3$ , pH 6–11) containing  $\text{NaOH-H}_3\text{PO}_4$  (0.1  $\text{mol dm}^{-3}$ ) and poly[2-(dimethylamino)hexanamide] (PDAH) (0.04 g). Dark brown aqueous PDAH solution (Cluster Conc: 1.5 mM) thus prepared was used for measurements.

**Physical Measurements.** Electronic absorption spectra were obtained by a Shimadzu UV-265FW spectrophotometer. Cyclic voltammetry measurements were performed with a BAS CV-50W electrochemical analyzer using a glassy carbon electrode in DMF and an indium–tin oxide (ITO) electrode in aqueous PDAH solutions, respectively.  $\text{Et}_4\text{NClO}_4$  (0.1  $\text{mol dm}^{-3}$ ) and  $\text{NaOH-H}_3\text{PO}_4$  (0.1  $\text{mol dm}^{-3}$ ) were used as supporting electrolytes in DMF and in aqueous PDAH solutions, respectively. A saturated calomel electrode (SCE) was used as a reference. In the measurement in DMF, a reference electrode (SCE) was separated from the sample DMF solution by a Luggin capillary containing KCl. This capillary was positioned as close as possible to the working electrode to minimize  $iR$  drop.

## Results and Discussion

**Electronic Absorption Spectra of a Series of  $[\text{Fe}_4\text{X}_4(\text{YAd})_4]^{2-}$  ( $\text{X}, \text{Y} = \text{S}$  and  $\text{Se}$ ).** Figure 1 shows the electronic absorption spectra of  $[\text{Fe}_4\text{S}_4(\text{SeAd})_4]^{2-}$  in DMF (solid line) and in aqueous PDAH solutions at pH 7 (dotted line, see below), as a representative example of these clusters. All the clusters show two absorption maxima at around 310 and 420 nm in DMF (Table 1), which are assigned to charge-transfer transitions from the terminal sulfur or selenium atoms to the iron atoms of the  $\text{Fe}_4\text{X}_4$  ( $\text{X} = \text{S}$  and  $\text{Se}$ ) core.<sup>30</sup> In fact, the intensities of these absorption bands are mainly dependent on the difference in the AdS/AdSe terminal ligands rather than the alteration of the  $\text{Fe}_4\text{S}_4/\text{Fe}_4\text{Se}_4$  core. These results are consistent with prior observations in the series of  $[\text{Fe}_4\text{X}_4(\text{C}_6\text{H}_5)_4]^{2-}$  ( $\text{X}, \text{Y} = \text{S}$  and  $\text{Se}$ )<sup>30</sup> and  $[\text{Fe}_4\text{X}_4(\text{YR})_4]^{2-}$  ( $\text{X}, \text{Y} = \text{S}$  and  $\text{Se}$ ;  $\text{R} = n\text{-C}_{12}\text{H}_{25}$ ,  $\text{C}_6\text{H}_4\text{-}p\text{-}t\text{-Bu}$ ).<sup>31</sup> Poly[2-(dimethylamino)hexanamide] (PDAH) was used to solubilize  $[\text{Fe}_4\text{X}_4(\text{YAd})_4]^{2-}$  ( $\text{X}, \text{Y} = \text{S}$  and  $\text{Se}$ ) in aqueous solutions, in which these clusters also show two absorption maxima at almost the same positions in DMF. Although the absorption bands of these clusters in aqueous PDAH solutions are slightly broad compared to those in DMF, electronic absorption spectra of the clusters in aqueous PDAH solutions (pH 7.0) were almost unchanged at 20 °C for 4 h. Even the fully selenium-substituted  $[\text{Fe}_4\text{Se}_4(\text{SeAd})_4]^{2-}$  maintained the 90% intensity of the original spectrum at 420 nm for 4 h. Thus, the hydrolysis of  $[\text{Fe}_4\text{X}_4(\text{YAd})_4]^{2-}$  is effectively depressed in aqueous PDAH solutions, where the clusters would be embedded in the polymer chains due to hydrogen bondings between  $\text{Fe}_4\text{X}_4$  ( $\text{X} = \text{S}$  and  $\text{Se}$ ) or YAd ( $\text{Y} = \text{S}$  and  $\text{Se}$ ) and amino or amide groups of PDAH. Indeed, the high stability of Fds<sup>32</sup> and HiPIPs,<sup>9,10</sup> in  $\text{H}_2\text{O}$  is ascribed to hydrogen bondings between terminal and/or core sulfur and peptide NH protons in hydrophobic spheres.

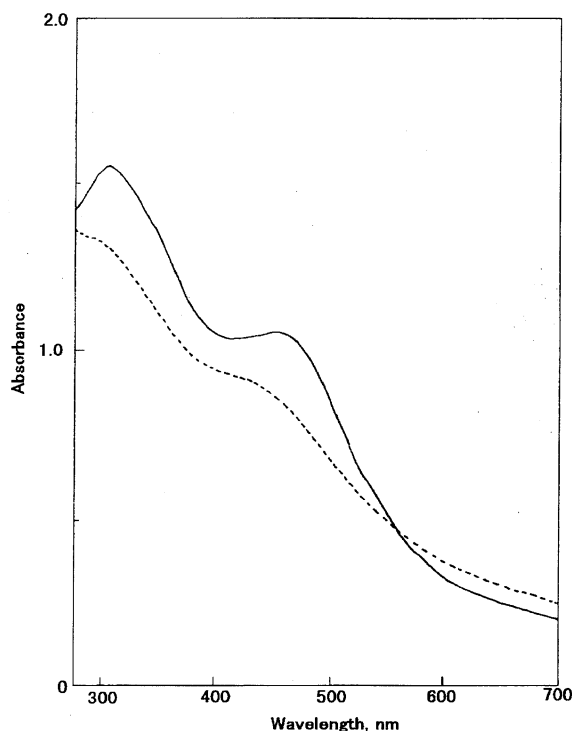


Fig. 1. Electronic absorption spectra of  $[\text{Fe}_4\text{S}_4(\text{SeAd})_4]^{2-}$  in DMF (solid line) (Concn  $1.10 \times 10^{-3}$  M using a 0.1 cm cell) and in aqueous PDAH solution at pH 7 (dotted line) (Concn  $1.01 \times 10^{-4}$  M with a 1.0 cm cell) ( $1 \text{ M} = 1 \text{ mol dm}^{-3}$ ).

Table 1. Electronic Spectral Data for the  $[\text{Fe}_4\text{X}_4(\text{YAd})_4]^{2-}$  (X, Y = S and Se) in DMF and in Aqueous PDAH Solutions

Cluster	$\lambda_{\text{max}}/\text{nm}$ ( $\epsilon/\text{M}^{-1} \text{cm}^{-1}$ )	
	in DMF	in aq PDAH
$[\text{Fe}_4\text{S}_4(\text{SAd})_4]^{2-}$	297 (23100)	290 (19900)
	419 (16700)	410 (10900)
$[\text{Fe}_4\text{S}_4(\text{SeAd})_4]^{2-}$	308 (14100)	296 (13400)
	444 (9740)	430 (9100)
$[\text{Fe}_4\text{Se}_4(\text{SAd})_4]^{2-}$	312 (18900)	300 (18300)
	420 (13800)	420 (10400)
$[\text{Fe}_4\text{Se}_4(\text{SeAd})_4]^{2-}$	310 (14600)	310 (sh)
	420 (8390)	420 (5390)

**Redox Behavior of  $[\text{Fe}_4\text{X}_4(\text{YAd})_4]^{2-}$  (X, Y = S and Se) in DMF and Aqueous Poly[2-(dimethylamino)hexanamide] (PDAH) Solutions.** We have reported that cyclic

voltammograms of  $[\text{Fe}_4\text{X}_4(\text{YAd})_4]^{2-}$  (X, Y = S and Se; R =  $n\text{-C}_{12}\text{H}_{25}$  and  $\text{C}_6\text{H}_4\text{-}p\text{-}t\text{-Bu}$ ) show reversible  $[\text{Fe}_4\text{X}_4]^{+/2+}$  redox couples in the range  $E_{1/2} = -0.94$  to  $-1.37$  V vs. SCE in DMF, but those clusters displayed a strong irreversible oxidation wave of  $[\text{Fe}_4\text{X}_4(\text{YAd})_4]^{2-}$  (X, Y = S and Se; R =  $n\text{-C}_{12}\text{H}_{25}$  and  $\text{C}_6\text{H}_4\text{-}p\text{-}t\text{-Bu}$ ) around 0 V.<sup>31)</sup> On the contrary,  $[\text{Fe}_4\text{S}_4(\text{SAd})_4]^{2-}$  undergoes the reversible not only  $[\text{Fe}_4\text{S}_4]^{+/2+}$  but also  $[\text{Fe}_4\text{S}_4]^{2+/3+}$  redox reactions at  $E_{1/2} = -1.34$  and  $-0.10$  V vs. SCE, respectively, in the same solvent (Table 2).<sup>23,24)</sup> Similarly, the remaining three selenium-substituted clusters  $[\text{Fe}_4\text{X}_4(\text{YAd})_4]^{2-}$  (X, Y = S, Se; Se, S; Se, Se) exhibited the pseudo-reversible  $[\text{Fe}_4\text{X}_4]^{+/2+}$  and  $[\text{Fe}_4\text{X}_4]^{2+/3+}$  redox couples in the range  $E_{1/2} = -1.28$  to  $-1.35$  V vs. SCE and  $E_{1/2} = -0.17$  to  $-0.20$  V vs. SCE, respectively, as shown in Table 2, where  $E_{1/2}$  is approximated by the average of the cathodic and anodic peak potentials. As a typical example, the voltammogram of  $[\text{Fe}_4\text{S}_4(\text{SeAd})_4]^{2-}$  in DMF is shown in Fig. 2. The anodic peak current of the  $[\text{Fe}_4\text{X}_4]^{2+/3+}$  couple decreased in the order;  $[\text{Fe}_4\text{S}_4(\text{SAd})_4]^{2-} \gg [\text{Fe}_4\text{S}_4(\text{SeAd})_4]^{2-} \approx [\text{Fe}_4\text{Se}_4(\text{SAd})_4]^{2-} > [\text{Fe}_4\text{Se}_4(\text{SeAd})_4]^{2-}$  in DMF, and the peak current ratio

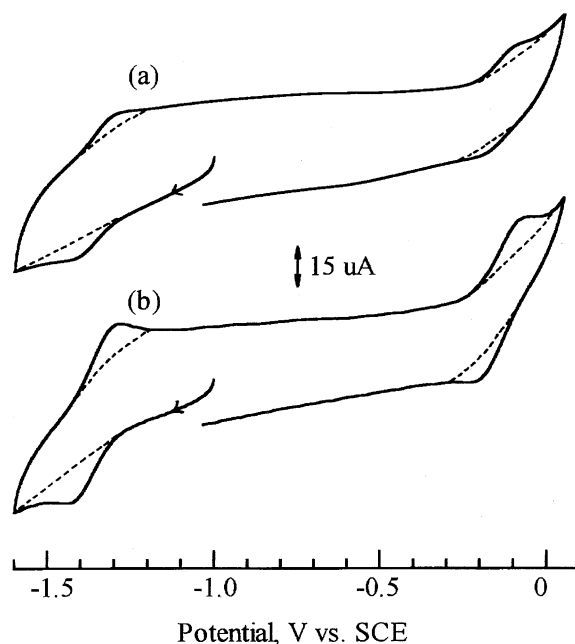


Fig. 2. Cyclic voltammograms of  $[\text{Fe}_4\text{S}_4(\text{SeAd})_4]^{2-}$  in DMF; (a) in the absence of AdSeH and (b) in the presence of 40 times excess of AdSeH; scan rate  $0.1 \text{ V s}^{-1}$ .

Table 2. Electrochemical Parameters of  $[\text{Fe}_4\text{X}_4(\text{YAd})_4]^{2-}$  (X, Y = S, Se; Ad = 1-Adamantyl) in DMF and in Aqueous PDAH Solutions

Cluster	$E_{1/2}/\text{V}$ vs. SCE					
	in DMF		in aq PDAH soln			
	(3-/2-)	(2-/1-)	(3-/2-)	pH	(2-/1-)	pH
$[\text{Fe}_4\text{S}_4(\text{SAd})_4]^{2-}$	-1.34	-0.10	-0.90	7.08	-0.28	7.08
$[\text{Fe}_4\text{S}_4(\text{SeAd})_4]^{2-}$	-1.35	-0.17	-0.87	7.08	-0.21	7.08
$[\text{Fe}_4\text{Se}_4(\text{SAd})_4]^{2-}$	-1.28	-0.18	-0.89	7.03	-0.28	7.00
$[\text{Fe}_4\text{Se}_4(\text{SeAd})_4]^{2-}$	-1.29	-0.20	-0.89	7.08	-0.25	6.99

$I_c/I_a$  of  $[\text{Fe}_4\text{X}_4]^{2+/3+}$  couple showed the similar tendency of  $I_c/I_a = 0.9$  to  $0.4$ . The voltammetry of the selenium-substituted clusters was also conducted in the presence of excess ligands to examine dissociation of the terminal ligand in DMF. In fact, the  $I_c/I_a$  value of the  $[\text{Fe}_4\text{S}_4(\text{SeAd})_4]^{3-/2-/-}$  redox couple was increased to  $0.85$  from  $0.6$  by an addition of 40 times excess of AdSeH (Fig. 2b). Other two selenium-substituted clusters also afforded the pseudo-reversible  $[\text{Fe}_4\text{X}_4(\text{YAd})_4]^{2-/1-}$  ( $\text{X}, \text{Y} = \text{S}, \text{Se}; \text{Se}, \text{Se}$ ) redox couples in the presence of excess ligand. Such behavior is explained by depression of dissociation of terminal ligands from both  $[\text{Fe}_4\text{X}_4(\text{YAd})_4]^{2-}$  and  $[\text{Fe}_4\text{X}_4(\text{YAd})_4]^{-}$  ( $\text{X}, \text{Y} = \text{S}, \text{Se}; \text{Se}, \text{S}; \text{Se}, \text{Se}$ ) by an addition of free ligands.

The cyclic voltammograms of  $[\text{Fe}_4\text{S}_4(\text{YAd})_4]^{2-}$  ( $\text{Y} = \text{S}$  and  $\text{Se}$ ) in aqueous PDAH solutions (pH 7.0) showed the cathodic and anodic waves of the  $[\text{Fe}_4\text{S}_4(\text{YAd})_4]^{2-/1-}$  couple as shown in Fig. 3, while those of the  $[\text{Fe}_4\text{S}_4(\text{YAd})_4]^{3-/2-/-}$  one were scarcely detected by an ITO electrode. On the other hand, the cathodic and anodic waves of the  $[\text{Fe}_4\text{S}_4(\text{YAd})_4]^{3-/2-}$  couple emerged clearly when  $[\text{Fe}_4\text{S}_4(\text{YAd})_4]^{3-}$  ( $\text{Y} = \text{S}$  and  $\text{Se}$ ) had been adsorbed on the surface of the ITO electrode by applying the potential at  $-1.0$  V (vs. SCE) to the electrode for 20–30 s (Fig. 3). Under these conditions, both the  $[\text{Fe}_4\text{S}_4(\text{YAd})_4]^{3-/2-}$  and  $[\text{Fe}_4\text{S}_4(\text{YAd})_4]^{2-/1-}$  ( $\text{Y} = \text{S}$  and  $\text{Se}$ ) redox couples stably appeared as pseudo-reversible waves even in multi-potential scanning, though the peak currents of the former were still lower than the latter. The cathodic and anodic peak currents of the  $[\text{Fe}_4\text{S}_4(\text{YAd})_4]^{3-/2-}$  and  $[\text{Fe}_4\text{S}_4(\text{YAd})_4]^{2-/1-}$  ( $\text{Y} = \text{S}$  and  $\text{Se}$ ) were proportional to first order and one-half order, respectively, with respect to the scanning rates in the range of 20–600  $\text{mV s}^{-1}$ . Thus, the  $[\text{Fe}_4\text{S}_4(\text{YAd})_4]^{2-}$  adsorbed on the surface of an ITO working electrode undergoes one-

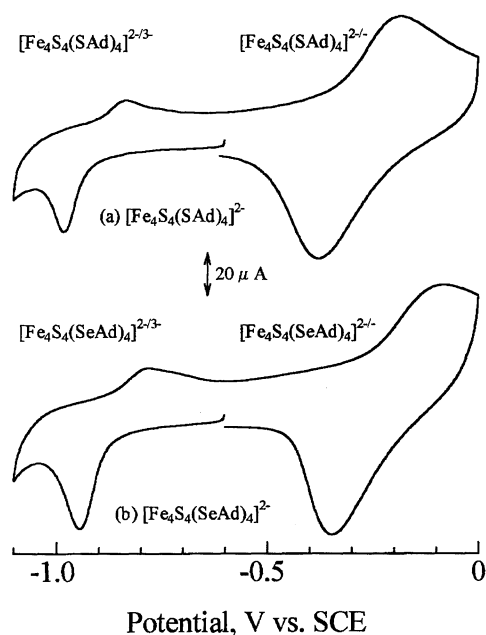


Fig. 3. Cyclic voltammograms of (a)  $[\text{Fe}_4\text{S}_4(\text{SAd})_4]^{2-}$  and (b)  $[\text{Fe}_4\text{S}_4(\text{SeAd})_4]^{2-}$  in aqueous PDAH solutions at pH 7.08; scan rate  $0.1 \text{ V s}^{-1}$ .

electron reduction in the aqueous PDAH solution, while the redox process of the  $[\text{Fe}_4\text{S}_4(\text{YAd})_4]^{2-/1-}$  ( $\text{Y} = \text{S}$  and  $\text{Se}$ ) couple is concluded to be a diffusion-controlled reaction. Such a difference may be caused by competitive adsorption among the PDAH, (3-), (2-), and (1-) states of the clusters at different pHs.<sup>24)</sup> Other clusters  $[\text{Fe}_4\text{Se}_4(\text{YAd})_4]^{2-}$  ( $\text{Y} = \text{S}$  and  $\text{Se}$ ) also afford similar behavior in aqueous PDAH solutions. The redox potential of  $[\text{Fe}_4\text{S}_4(\text{SC}_6\text{H}_4\text{-}p\text{-C}_8\text{H}_{17})_4]^{2-}$  adsorbed on Hg appears 80 mV more positive than that of the cluster dissolved in aqueous lecithin solutions,<sup>32)</sup> but the  $\text{p}K_a$  of the one-electron reduced cluster was not affected by the adsorption (see below).

$E_{1/2}$  values of the  $[\text{Fe}_4\text{X}_4(\text{YAd})_4]^{3-/2-}$  and  $[\text{Fe}_4\text{X}_4(\text{YAd})_4]^{2-/1-}$  couple ( $\text{X}, \text{Y} = \text{S}$  and  $\text{Se}$ ) in aqueous PDAH solutions at pH ca. 7 are shown in Table 2 together with those in DMF. Apparently, both the  $E_{1/2}$  values of the  $[\text{Fe}_4\text{X}_4(\text{YAd})_4]^{3-/2-}$  ( $E_{1/2} = -0.8$ — $-0.9$  V) and  $[\text{Fe}_4\text{X}_4(\text{YAd})_4]^{2-/1-}$  couple ( $E_{1/2} = -0.2$ — $-0.3$  V) are close to those of Fds<sup>4,33)</sup> and HiPIPs,<sup>8)</sup> respectively. It should be noticed that pseudo-reversible  $[\text{Fe}_4\text{X}_4(\text{YAd})_4]^{2-/1-}$  ( $\text{X}, \text{Y} = \text{S}$  and  $\text{Se}$ ) redox couples are observed in aqueous PDAH solutions even in the absence of free ligand in contrast to the redox reactions in DMF described above. This fact indicates that  $[\text{Fe}_4\text{X}_4(\text{YAd})_4]^{2-}$  undergoes one-electron redox reaction in aqueous PDAH solution without dissociation of the terminal ligand. Protection of both the oxidized  $[\text{Fe}_4\text{X}_4(\text{YAd})_4]^{2-}$  and super-oxidized  $[\text{Fe}_4\text{X}_4(\text{YAd})_4]^{-}$  ( $\text{X}, \text{Y} = \text{S}$  and  $\text{Se}$ ) from hydrolysis reactions by PDAH is probably due to the interaction of both amino and amide groups with terminal and/or core sulfur and selenium atoms in the clusters.

**Protonation Behavior of  $[\text{Fe}_4\text{X}_4(\text{YAd})_4]^{2-}$  ( $\text{X}, \text{Y} = \text{S}$  and  $\text{Se}$ ) in Aqueous PDAH Solutions.** The  $E_{1/2}$  values of the  $[\text{Fe}_4\text{X}_4(\text{YAd})_4]^{3-/2-}$  and  $[\text{Fe}_4\text{X}_4(\text{YAd})_4]^{2-/1-}$  redox couples in aqueous PDAH solutions at various pHs are given in Fig. 4. All the  $E_{1/2}$  values of the  $[\text{Fe}_4\text{X}_4(\text{YAd})_4]^{3-/2-}$  ( $\text{X}, \text{Y} = \text{S}$  and  $\text{Se}$ ) couples are cathodically shifted with increasing pH, while the  $E_{1/2}$  values have a tendency to level off from each linear relation on both the alkaline and acidic sides. Such characteristic pH dependence of the  $E_{1/2}$  is interpreted in terms of a protonation/de-protonation equilibrium both of the oxidized  $[\text{Fe}_4\text{X}_4(\text{YAd})_4]^{2-}$  and of the reduced  $[\text{Fe}_4\text{X}_4(\text{YAd})_4]^{3-}$  ( $\text{X}, \text{Y} = \text{S}$  and  $\text{Se}$ ) in aqueous PDAH solutions.<sup>24,34)</sup> The one proton participation in the redox reaction of the  $[\text{Fe}_4\text{X}_4(\text{YAd})_4]^{3-/2-}$  ( $\text{X}, \text{Y} = \text{S}$  and  $\text{Se}$ ) couple is rationalized on the basis of the slope of the linear relation of  $d(E_{1/2})/d(\text{pH}) = \text{ca. } -70 \text{ mV}$ , although the values of  $d(E_{1/2})/d(\text{pH})$  are somewhat larger than the theoretical values of  $\text{H}^+/\text{e}^-$  transfer ( $-63 \text{ mV}$ ).<sup>35)</sup>

In the case of  $[\text{Fe}_4\text{X}_4(\text{YAd})_4]^{2-/1-}$  ( $\text{X}, \text{Y} = \text{S}$  and  $\text{Se}$ ) redox couples, all the  $E_{1/2}$  values are also cathodically shifted in a linear fashion with increasing pH. One proton is similarly expected to participate in the  $[\text{Fe}_4\text{X}_4(\text{YAd})_4]^{2-/1-}$  redox reactions in aqueous PDAH solutions. The  $E_{1/2}$  of the  $[\text{Fe}_4\text{X}_4(\text{YAd})_4]^{2-/1-}$  couple become pH independent around pH 7 or 8, where oxidation and reduction reactions involve no net proton exchange. Thus, redox-linked protonation occurs

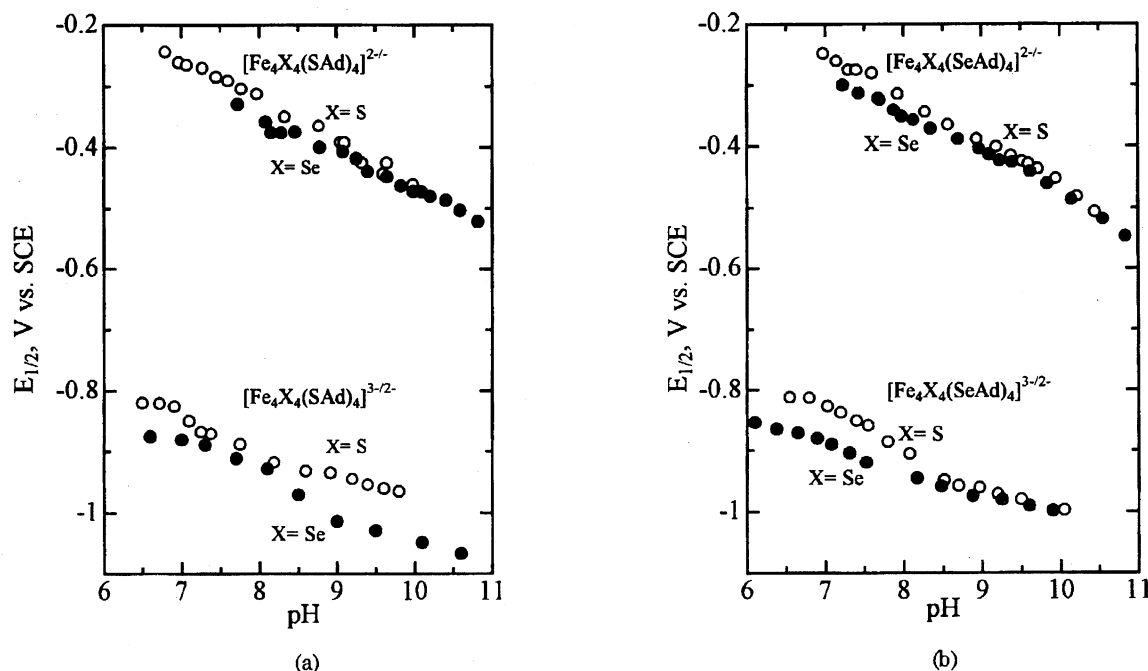


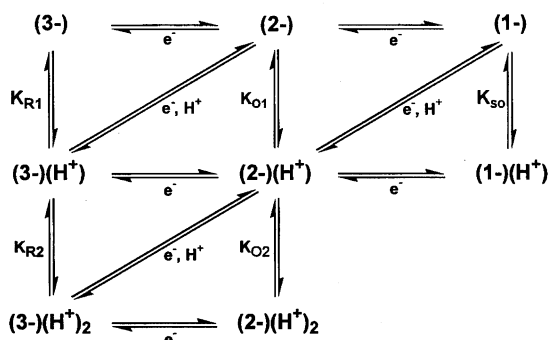
Fig. 4.  $E_{1/2}$  values of the redox couples at various pHs in aqueous PDAH solutions at 20 °C; (a)  $[\text{Fe}_4\text{X}_4(\text{SAd})_4]^{3-/2-}$  and  $[\text{Fe}_4\text{X}_4(\text{SAd})_4]^{2-/}$  [X = S (○) and Se (●)] and (b)  $[\text{Fe}_4\text{X}_4(\text{SeAd})_4]^{3-/2-}$  and  $[\text{Fe}_4\text{X}_4(\text{SeAd})_4]^{2-/}$  [X = S (○) and Se (●)].

in both the  $[\text{Fe}_4\text{X}_4(\text{YAd})_4]^{3-/2-}$  and  $[\text{Fe}_4\text{X}_4(\text{YAd})_4]^{2-/}$  redox processes in aqueous PDAH solutions.

We have reported that the first and second protonation reactions of  $[\text{Fe}_4\text{S}_4(\text{SAd})_4]^{2-}$  take place around pH 10.5 and 7 (Eqs. 1 and 2), based on titration of the aqueous PDAH solution of  $[\text{Fe}_4\text{S}_4(\text{SAd})_4]^{2-}$  by diluted  $\text{H}_2\text{SO}_4$ .<sup>24)</sup> Similar pH dependence of the  $E_{1/2}$  values of the  $[\text{Fe}_4\text{X}_4(\text{YAd})_4]^{3-/2-}$  and  $[\text{Fe}_4\text{X}_4(\text{YAd})_4]^{2-/}$  couples strongly indicates that the first and second protonation reactions also occur in the clusters  $[\text{Fe}_4\text{X}_4(\text{YAd})_4]^{2-}$  (X, Y = S and Se). Therefore, possible redox-linked protonation of the  $[\text{Fe}_4\text{X}_4(\text{YAd})_4]^{2-/}$  as well as  $[\text{Fe}_4\text{X}_4(\text{YAd})_4]^{3-/2-}$  redox couples can be considered as shown in Scheme 2, where  $[\text{Fe}_4\text{X}_4(\text{YAd})_4]^{n-}$  cluster ( $n = 1-3$ ) is abbreviated as  $(n-)$  and  $K_{R1}$ ,  $K_{R2}$ ,  $K_{O1}$ ,  $K_{O2}$ , and  $K_{S0}$  express the dissociation constants of protonated clusters  $(3-)(\text{H}^+)$ ,  $(3-)(\text{H}^+)_2$ ,  $(2-)(\text{H}^+)$ ,  $(2-)(\text{H}^+)_2$  and  $(1-)(\text{H}^+)$ , respectively. Based on the electron density of the clusters in the three oxidation states, protonation takes place in the order  $[\text{Fe}_4\text{X}_4(\text{YAd})_4]^{3-} > [\text{Fe}_4\text{X}_4(\text{YAd})_4]^{2-} > [\text{Fe}_4\text{X}_4(\text{YAd})_4]^{-}$ . Since the first protonation of the oxi-

dized form of  $[\text{Fe}_4\text{S}_4(\text{SAd})_4]^{2-}$  occurs over pH 10.5 as previously reported,<sup>24)</sup> the reduced  $[\text{Fe}_4\text{X}_4(\text{YAd})_4]^{3-}$  and oxidized  $[\text{Fe}_4\text{X}_4(\text{YAd})_4]^{2-}$  forms must undergo the first protonation over pH 10.5. As representative examples, redox reactions of the  $[\text{Fe}_4\text{S}_4(\text{SAd})_4]^{3-/2-}$  and  $[\text{Fe}_4\text{Se}_4(\text{SeAd})_4]^{3-/2-}$  couples are taken up for consideration in Fig. 5. These Pourbaix diagrams show that two turning points appear both in acidic and alkaline regions in  $[\text{Fe}_4\text{X}_4(\text{YAd})_4]^{3-/2-}$  (X, Y = S, S; Se, Se) redox reaction, but only one turning point is observed in neutral region in the case of the  $[\text{Fe}_4\text{X}_4(\text{YAd})_4]^{2-/}$  (X, Y = S, S; Se, Se) redox reaction. If the first protonation reaction of the reduced form  $[\text{Fe}_4\text{X}_4(\text{YAd})_4]^{3-}$  and the oxidized form  $[\text{Fe}_4\text{X}_4(\text{YAd})_4]^{2-}$  occur over pH 10.5, the turning points of the  $[\text{Fe}_4\text{S}_4(\text{SAd})_4]^{3-/2-}$  redox reaction at pH 9.5 and of the  $[\text{Fe}_4\text{Se}_4(\text{SeAd})_4]^{3-/2-}$  one at pH 9 are reasonably assigned to  $\text{p}K_{R2}$  of di-protonated species  $[\text{Fe}_4\text{X}_4(\text{YAd})_4]^{3-}(\text{H}^+)_2$  (X, Y = S, S; Se, Se), respectively. Similarly, the turning points of the  $[\text{Fe}_4\text{X}_4(\text{YAd})_4]^{3-/2-}$  redox reactions at ca. 7 (X, Y = S, S) and ca. 6.5 (X, Y = Se, Se) correspond to  $\text{p}K_{O2}$  of di-protonated species  $[\text{Fe}_4\text{X}_4(\text{YAd})_4]^{2-}(\text{H}^+)_2$  (X, Y = S, S; Se, Se), respectively.<sup>24,34)</sup>

In similar manner, the protonation behavior of the  $[\text{Fe}_4\text{X}_4(\text{YAd})_4]^{2-/}$  (X, Y = S, S; Se, Se) redox couples is explained. The pH dependent regions above pH 7.2 (X, Y = S, S) and pH 8.2 (X, Y = Se, Se) correspond to the redox reactions between the mono-protonated cluster  $[\text{Fe}_4\text{X}_4(\text{YAd})_4]^{2-}(\text{H}^+)$  and non-protonated  $[\text{Fe}_4\text{X}_4(\text{YAd})_4]^{-}$  (X, Y = S, S; Se, Se), exchanging a net one proton. The turning points at around pH 7.2 (X, Y = S, S) and pH 8.2 (X, Y = Se, Se) afford the  $\text{p}K_{S0}$  of the protonated  $[\text{Fe}_4\text{X}_4(\text{YAd})_4]^{-}(\text{H}^+)$  (X, Y = S, S; Se, Se) and the turning points at around pH 6.8 (X, Y = S, S) and pH 6.4 (X, Y = Se, Se) mean the  $\text{p}K_{O2}$  of the di-protonated species,



Scheme 2.

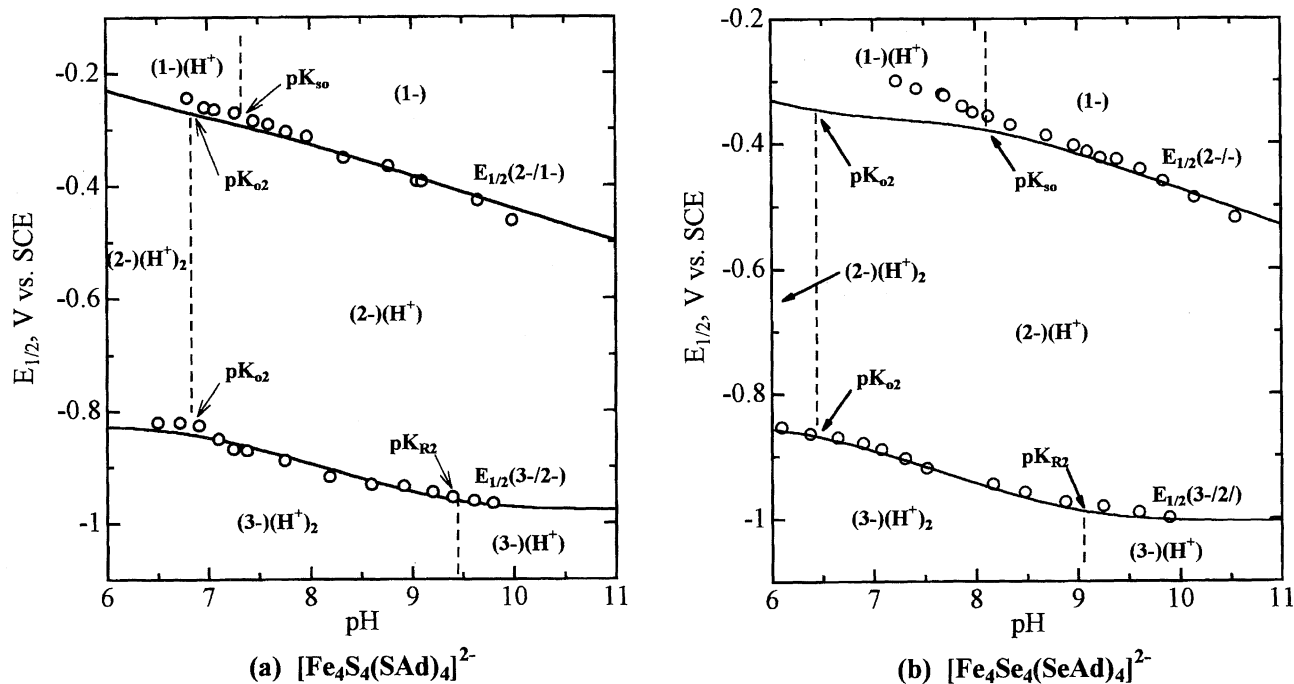


Fig. 5. Calculated  $E_{1/2}$  values (solid lines) of the  $[\text{Fe}_4\text{X}_4(\text{YAd})_4]^{3-/2-}$  and  $[\text{Fe}_4\text{X}_4(\text{YAd})_4]^{2-/1-}$  ( $\text{X}, \text{Y} = \text{S}, \text{S}; \text{Se}, \text{Se}$ ) redox couples at various pHs in aqueous PDAH solution together with the observed  $E_{1/2}$  values (circles).

$[\text{Fe}_4\text{X}_4(\text{YAd})_4]^{2-}(\text{H}^+)_2$  ( $\text{X}, \text{Y} = \text{S}, \text{S}; \text{Se}, \text{Se}$ ), respectively. Thus,  $[\text{Fe}_4\text{X}_4(\text{YAd})_4]^-$  ( $\text{X}, \text{Y} = \text{S}, \text{S}; \text{Se}, \text{Se}$ ) may exist as non-protonated species in alkaline region, but protonation takes place below pH 7.2 ( $\text{X}, \text{Y} = \text{S}, \text{S}$ ) and pH 8.2 ( $\text{X}, \text{Y} = \text{Se}, \text{Se}$ ) as shown in Fig. 5. Analogous phase diagrams have been accomplished for other two clusters  $[\text{Fe}_4\text{S}_4(\text{SeAd})_4]^{2-}$  and  $[\text{Fe}_4\text{Se}_4(\text{SAd})_4]^{2-}$ , leading us to evaluate basicity of the clusters in the three oxidation state in aqueous PDAH solutions.

**Determination of Basicity of  $\text{Fe}_4\text{X}_4$  ( $\text{X} = \text{S}$  and  $\text{Se}$ ) Cores and Terminal YAd ( $\text{Y} = \text{S}$  and  $\text{Se}$ ) Ligands.** On the basis of multi-step protonation of these clusters as shown in Scheme 2, the half-wave potentials  $E(3-/2-)$  and  $E(2-/1-)$  for the overall electrode reactions, therefore, can be written as Eqs. 3 and 4, where  $R$ ,  $T$ , and  $F$  are the gas constant, temperature, and the Faraday constant, respectively. Thus,  $E(3-/2-)$  and  $E(2-/1-)$  were calculated by Eqs. 3 and 4, using  $pK_{R1}$ ,  $pK_{R2}$ ,  $pK_{O1}$ ,  $pK_{O2}$ ,  $pK_{SO}$ , and  $E^\circ$  values listed in

Table 3. Computer simulation curves of the  $E(3-/2-)$  values of  $[\text{Fe}_4\text{X}_4(\text{YAd})_4]^{2-}$  ( $\text{X}, \text{Y} = \text{S}, \text{S}; \text{Se}, \text{Se}$ ) calculated by Eq. 3 (solid lines in Fig. 5) give reasonable agreement with the observed  $E_{1/2}$  values. Similarly, the calculated  $E(2-/1-)$  values of the  $[\text{Fe}_4\text{X}_4(\text{YAd})_4]^{2-}$  ( $\text{X}, \text{Y} = \text{S}, \text{S}; \text{Se}, \text{Se}$ ) by Eq. 3 appear to be consistent with the observed values, but the observed  $E_{1/2}$  values of the fully selenium-substituted cluster tend to anodically deviate from the calculated lines at pH below 8, which may be affected by the adsorption phenomenon of the super-oxidized species of the clusters on the surface of an ITO electrode as described above. Calculation of  $E_{1/2}$  values by computer using the Eqs. 3 or 4 with  $pK_{R1}$ ,  $pK_{R2}$ ,  $pK_{O1}$ ,  $pK_{O2}$ ,  $pK_{SO}$ , and  $E^\circ$  values listed in Table 3 agrees with the experimental values of the clusters  $[\text{Fe}_4\text{X}_4(\text{YAd})_4]^{2-}$  ( $\text{X}, \text{Y} = \text{S}, \text{S}; \text{Se}, \text{Se}$ ) as shown by solid lines in Fig. 5. The parameters listed in Table 3 are the most suitable values which give the best curve fittings for all the

Table 3.  $pK$  Values of the Reduced, Oxidized, and Super-oxidized Forms of  $[\text{Fe}_4\text{X}_4(\text{YAd})_4]^{2-}$  in Aqueous PDAH Solution

Cluster	$pK_{R1}$		$pK_{R2}$		$pK_{O1}$		$pK_{O2}$		$pK_{SO}$		$E^\circ$ V vs. SCE
	Obsd	Calcd	Obsd	Calcd	Obsd	Calcd	Obsd	Calcd	Obsd	Calcd	
$[\text{Fe}_4\text{S}_4(\text{SAd})_4]^{2-}$	—	12.7	9.4	9.5	—	13.8	6.8	6.8	—	—	-0.915 <sup>a)</sup>
						13.8		6.9	7.2	7.3	-0.661 <sup>b)</sup>
$[\text{Fe}_4\text{S}_4(\text{SeAd})_4]^{2-}$	—	12.7	9.5	9.5	—	13.8	6.5	6.4	—	—	-0.92 <sup>a)</sup>
						13.9		6.4	7.4	7.4	-0.675 <sup>b)</sup>
$[\text{Fe}_4\text{Se}_4(\text{SAd})_4]^{2-}$	—	12.4	8.9	9.1	—	13.5	7.0	6.9	—	—	-0.955 <sup>a)</sup>
						13.4		6.9	8.3	8.2	-0.678 <sup>b)</sup>
$[\text{Fe}_4\text{Se}_4(\text{SeAd})_4]^{2-}$	—	12.4	8.9	9.0	—	13.4	6.4	6.3	—	—	-0.955 <sup>a)</sup>
						13.4		6.4	8.2	8.1	-0.67 <sup>b)</sup>

a)  $E^\circ$  in Eq. 3. b)  $E^\circ$  in Eq. 4.

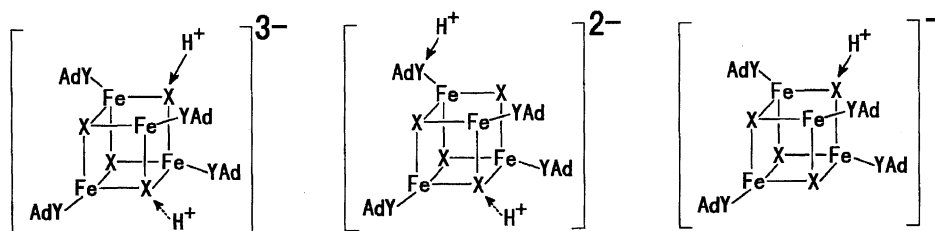


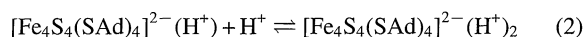
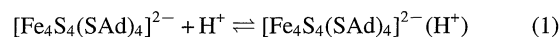
Fig. 6. Protonation behavior of the reduced, oxidized, and super-oxidized forms of the  $[\text{Fe}_4\text{X}_4(\text{YAd})_4]^{2-}$  ( $\text{X}, \text{Y} = \text{S}, \text{Se}$ ) in aqueous PDAH solutions; solid arrows experimentally determined for the second protonation; dotted arrows estimated by computer simulation for the first protonation.

clusters.

Although no information on the  $\text{p}K_{\text{R1}}$  values of  $[\text{Fe}_4\text{X}_4(\text{YAd})_4]^{3-}(\text{H}^+)$  and  $\text{p}K_{\text{O1}}$  values of  $[\text{Fe}_4\text{X}_4(\text{YAd})_4]^{2-}(\text{H}^+)$  were obtained by experiment, the first protonation reactions of  $[\text{Fe}_4\text{X}_4(\text{YAd})_4]^{3-}$  and  $[\text{Fe}_4\text{X}_4(\text{YAd})_4]^{2-}$  probably take place at the  $\text{Fe}_4\text{X}_4$  ( $\text{X} = \text{S}$  and  $\text{Se}$ ) cores (Fig. 6), since the speculated  $\text{p}K_{\text{R1}}$  values for  $[\text{Fe}_4\text{X}_4(\text{YAd})_4]^{3-}(\text{H}^+)$  and  $\text{p}K_{\text{O1}}$  values for  $[\text{Fe}_4\text{X}_4(\text{YAd})_4]^{2-}(\text{H}^+)$  (Table 3) are dependent on  $\text{Fe}_4\text{X}_4$  ( $\text{X} = \text{S}$  and  $\text{Se}$ ) cores. The  $\text{p}K_{\text{R2}}$  values of  $[\text{Fe}_4\text{X}_4(\text{YAd})_4]^{3-}(\text{H}^+)_2$  ( $\text{X}, \text{Y} = \text{S}$  and  $\text{Se}$ ) obtained by experiment and the computer simulation (Table 3) are divided into two groups depending on core  $\text{X}$ ; 9.5 for  $\text{X} = \text{S}$  and 8.9 for  $\text{X} = \text{Se}$ . On the other hand,  $\text{p}K_{\text{O2}}$  values of  $[\text{Fe}_4\text{X}_4(\text{YAd})_4]^{2-}(\text{H}^+)_2$  are classified to two groups by terminal  $\text{Y}$ ; 6.9 for  $\text{Y} = \text{S}$  and 6.4 for  $\text{Y} = \text{Se}$ . These results indicate that  $\text{p}K_{\text{R2}}$  values are controlled by the core sulfur and selenium atoms, while  $\text{p}K_{\text{O2}}$  values are influenced by the terminal sulfur and selenium atoms. Thus, the second protonation reactions of  $[\text{Fe}_4\text{X}_4(\text{YAd})_4]^{3-}(\text{H}^+)$  and  $[\text{Fe}_4\text{X}_4(\text{YAd})_4]^{2-}(\text{H}^+)$  take place in the  $\text{Fe}_4\text{X}_4$  core and in  $\text{YAd}$  ligands, respectively (Fig. 6).

The  $\text{p}K_{\text{SO}}$  values of  $[\text{Fe}_4\text{X}_4(\text{YAd})_4]^-$  obtained by experiment and the simulation (Table 3) are also divided into two groups; 7.4 for  $\text{X} = \text{S}$  and 8.2 for  $\text{X} = \text{Se}$ . The  $\text{p}K_{\text{SO}}$  values are dependent on the difference of the sulfur and the selenium atoms of the  $\text{Fe}_4\text{X}_4$  cores ( $\text{X} = \text{S}$  and  $\text{Se}$ ). Thus, the protonation of the super-oxidized cluster  $[\text{Fe}_4\text{X}_4(\text{YAd})_4]^-$  again takes place at sulfur or selenium of the  $\text{Fe}_4\text{X}_4$  core ( $\text{X} = \text{S}$  and  $\text{Se}$ ) in aqueous PDAH solutions as shown in Fig. 6.

In connection with hydrogen bonding in natural ferredoxins and HiPIPs, we conclude as follows. The synthetic cluster  $[\text{Fe}_4\text{X}_4(\text{YAd})_4]^{2-}$  ( $\text{X}, \text{Y} = \text{S}, \text{Se}$ ) exists as an equilibrium mixture with non-protonated and protonated species in aqueous PDAH solution. Redox-linked protonation behavior of  $[\text{Fe}_4\text{X}_4(\text{YAd})_4]^{2-}$  shows that the basicity of the core S atoms of the reduced, oxidized, and super-oxidized forms of  $[\text{Fe}_4\text{S}_4(\text{SR})_4]^{2-}$  in aqueous solution is stronger than that of the terminal S ligands and that basicity of the core S of the reduced species  $[\text{Fe}_4\text{X}_4(\text{YAd})_4]^{3-}(\text{H}^+)$  is still stronger than that of the terminal S ligand, while the basicity of the terminal S ligand in the oxidized form  $[\text{Fe}_4\text{X}_4(\text{YAd})_4]^{2-}(\text{H}^+)$  shows reverse trend. Thus,  $\text{NH-S}$  hydrogen bonding in natural Fds and HiPIPs is controlled by the basicity of core sulfur or terminal sulfur atoms of reduced, oxidized, and super-oxidized forms of active center  $[\text{Fe}_4\text{S}_4(\text{Cys})_4]^{2-}$  in the hydrophobic sphere.



$$E(3-/2-) = E^\circ - \frac{RT}{nF} \ln \frac{K_{\text{O1}}K_{\text{O2}}(K_{\text{R1}}K_{\text{R2}} + K_{\text{R2}}[\text{H}^+] + [\text{H}^+]^2)}{K_{\text{R1}}K_{\text{R2}}(K_{\text{O1}}K_{\text{O2}} + K_{\text{O2}}[\text{H}^+] + [\text{H}^+]^2)} \quad (3)$$

$$E(2-/1-) = E^\circ - \frac{RT}{nF} \ln \frac{K_{\text{SO}}(K_{\text{O1}}K_{\text{O2}} + K_{\text{O2}}[\text{H}^+] + [\text{H}^+]^2)}{K_{\text{O1}}K_{\text{O2}}(K_{\text{SO}} + [\text{H}^+])} \quad (4)$$

## References

- 1) a) D. C. Yoch, D.I. Arnon, and W. V. Sweeney, *J. Biol. Chem.*, **250**, 8330 (1975); b) H. Hiura, T. Kakuno, J. Yamashita, H. Matsubara, and T. Horio, *J. Biochem.*, **89**, 1787 (1981); c) K. T. S. Shanmugan, D. B. Buchanan, and D. E. Arnon, *Biochem. Biophys. Acta*, **256**, 477 (1972).
- 2) a) K. M. Werber and M. Mevarech, *Arch. Biochem. Biophys.*, **186**, 60 (1978); b) S. Seki, M. Hagiwara, K. Kudo, and M. Ishimoto, *J. Biochem.*, **85**, 833 (1979).
- 3) a) B. E. Smith, D. J. Lowe, and R. C. Bray, *Biochem. J.*, **137**, 169 (1974); b) M. Tanaka, M. Haniyu, K. T. Yasunobu, and L. E. Mortenson, *J. Biol. Chem.*, **252**, 7093 (1977); c) V. Sunderson and F. M. Ausubel, *J. Biol. Chem.*, **256**, 2808 (1981).
- 4) a) J. M. Berg and R. H. Holm, in "Iron-Sulfur Proteins," John Wiley and Sons, New York (1982), Vol. 4, Chap. 1; b) C. L. Hill, J. Renaud, R. H. Holm, and L. E. Mortenson, *J. Am. Chem. Soc.*, **99**, 2549 (1977).
- 5) a) R. G. Bartsch, *Methods Enzymol.*, **53**, 329 (1978); b) C. W. Carter, *J. Biol. Chem.*, **252**, 7802 (1977).
- 6) a) G. M. Jensen, A. Warshel, and P. J. Stephen, *Biochemistry*, **33**, 10911 (1994); b) L. Banci, I. Bertini, S. Ciurli, C. Luchinat, and R. Pierattell, *Inorg. Chim. Acta*, **240**, 251 (1995); c) L. Banci, I. Bertini, G. G. Savellini, and C. Luchinat, *Inorg. Chem.*, **35**, 4248 (1996).
- 7) R. H. Holm and J. A. Ibers, in "Iron-Sulfur Proteins," Academic Press, New York (1977), Vol. 3, Chap. 1.
- 8) R. H. Holm, S. Ciurli, and J. A. Weigei, in "Progress in Inorg. Chem.," John Wiley and Sons, New York (1990), Vol. 38, Chap. 1.
- 9) a) M. M. Benning, T. E. Meyer, I. Rayment, and H. M. Holden, *Biochemistry*, **33**, 2476 (1994); b) G. Backes, Y. Mino, T. M. Loehr, T. E. Meyer, M. A. Cusanovich, W. V. Sweeney, E. T. Adman, and J. Sanders-Loehr, *J. Am. Chem. Soc.*, **113**, 2055 (1991).
- 10) a) L. Banci, I. Bertini, F. Capozzi, P. Carloni, S. Ciurli, C. Luchinat, and M. Piccioli, *J. Am. Chem. Soc.*, **115**, 3431 (1993); b) D. Li, A. Agarwal, and J. A. Cowan, *Inorg. Chem.*, **35**, 1121 (1996).

- 11) I. Bertini, I. C. Felli, D. H. W. Kastrau, C. Luchinat, M. Piccioli, and M. S. Viezzoli, *Eur. J. Biochem.*, **225**, 703 (1994).
- 12) a) B. V. DePamphilis, B. A. Averill, T. Herskovitz, L. Que, Jr., and R. H. Holm, *J. Am. Chem. Soc.*, **96**, 4159 (1974); b) L. Que, Jr., J. R. Anglin, M. A. Bobrik, A. Davison, and R. H. Holm, *J. Am. Chem. Soc.*, **96**, 6042 (1974); c) G. Christou, P. M. Mascharak, W. H. Armstrong, G. C. Papaefthymiou, R. B. Frankel, and R. H. Holm, *J. Am. Chem. Soc.*, **104**, 2820 (1982); d) W. H. Armstrong, P. K. Mascharak, and R. H. Holm, *J. Am. Chem. Soc.*, **104**, 4373 (1982); e) R. E. Johnson, G. C. Papaefthymiou, R. B. Frankel, and R. H. Holm, *J. Am. Chem. Soc.*, **105**, 7280 (1983); f) G. Christou, C. D. Garner, R. M. Miller, C. E. Johnson, and J. D. Rush, *J. Chem. Soc., Dalton Trans.*, **1983**, 2363.
- 13) For example,  $[Fe_4S_4(SR)_4]^{2-}$  ( $R = n-C_{12}H_{25}$  and  $C_6H_4-p-t-Bu$ ) undergoes an irreversible oxidation around 0 V vs. SCE in DMF.
- 14) T. O'Sullivan and M. M. Millar, *J. Am. Chem. Soc.*, **107**, 4097 (1985).
- 15) N. Ueyama, T. Terakawa, T. Sugawara, M. Fuji, and A. Nakamura, *Chem. Lett.*, **1984**, 1287.
- 16) Y. Okuno, K. Uoto, O. Yonemitsu, and T. Tomohiro, *J. Chem. Soc., Chem. Commun.*, **1987**, 1018.
- 17) a) T. Yamamura, T. Watanabe, A. Kikuchi, M. Ushiyama, T. Kobayashi, and H. Hirota, *J. Phys. Chem.*, **99**, 5525 (1995); b) T. Yamamura, M. Arai, T. Yamane, T. Ukai, M. Ushiyama, and H. Hirota, *Bull. Chem. Soc. Jpn.*, **69**, 2221 (1996); c) T. Yamamura, T. Watanabe, A. Kikuchi, T. Yamane, M. Ushiyama, and H. Hirota, *Inorg. Chem.*, **36**, 4849 (1997).
- 18) a) T. Ueno, N. Ueyama, and A. Nakamura, *J. Chem. Soc., Dalton Trans.*, **1996**, 3859; b) N. Ueyama, Y. Yamada, T. Okamura, S. Kimura, and A. Nakamura, *Inorg. Chem.*, **35**, 6473 (1996).
- 19) N. Ueyama, T. Okamura, and A. Nakamura, *J. Chem. Soc., Chem. Commun.*, **1992**, 1019.
- 20) N. Ueyama, N. Nishikawa, Y. Yamada, T. Okamura, and A. Nakamura, *J. Am. Chem. Soc.*, **118**, 12826 (1996).
- 21) a) N. Ueyama, T. Okamura, and A. Nakamura, *J. Am. Chem. Soc.*, **114**, 8129 (1992); b) H. Oku, N. Ueyama, and A. Nakamura, *Inorg. Chem.*, **36**, 1504 (1997).
- 22) T. Okamura, N. Ueyama, A. Nakamura, E. W. Ainscough, A. M. Brodie, and J. M. Waters, *J. Chem. Soc., Chem. Commun.*, **1993**, 1658.
- 23) a) M. Nakamoto, K. Tanaka, and T. Tanaka, *J. Chem. Soc., Chem. Commun.*, **1988**, 1422; b) H. Kambayashi, M. Nakamoto, S.-M. Peng, H. Nagao, and K. Tanaka, *Chem. Lett.*, **1992**, 919.
- 24) H. Kambayashi, H. Nagao, K. Tanaka, M. Nakamoto, and S.-M. Peng, *Inorg. Chim. Acta*, **209**, 143 (1993).
- 25) K. K. Khullar and L. Bauer, *J. Org. Chem.*, **36**, 3038 (1971).
- 26) J. M. Kokosa, L. Bauer, and R. S. Egan, *J. Org. Chem.*, **40**, 3196 (1975).
- 27) B. A. Averill, T. Herskovitz, R. H. Holm, and J. A. Ibers, *J. Am. Chem. Soc.*, **95**, 3523 (1973).
- 28) G. Christou, B. Ridge, and H. N. Rydon, *J. Chem. Soc., Dalton Trans.*, **1978**, 1423.
- 29) a) L. Que, Jr., M. A. Bobrik, J. A. Ibers, and R. H. Holm, *J. Am. Chem. Soc.*, **96**, 4168 (1974); b) L. Que, Jr., J. R. Anglin, M. A. Bobrik, A. Davison, and R. H. Holm, *J. Am. Chem. Soc.*, **96**, 6042 (1974).
- 30) M. A. Bobrik, E. J. Laskowski, R. W. Johnson, W. O. Gillum, J. M. Berg, K. O. Hodgson, and R. H. Holm, *Inorg. Chem.*, **17**, 1402 (1978).
- 31) M. Nakamoto and T. Tanaka, unpublished data.
- 32) K. Tanaka, M. Masanaga, and T. Tanaka, *J. Am. Chem. Soc.*, **108**, 5452 (1986).
- 33) a) E. T. Lode, C. L. Murray, and J. C. Rabinowitz, *J. Biol. Chem.*, **251**, 1683 (1976); b) J. C. Rabinowitz and W. V. Sweeney, *Annu. Rev. Biochem.*, **49**, 139 (1980); c) E. Adman, K. D. Watenpugh, and L. H. Jensen, *Proc. Natl. Acad. Sci. U.S.A.*, **72**, 4854 (1975).
- 34) a) M. Nakamoto, K. Tanaka, and T. Tanaka, *J. Chem. Soc., Chem. Commun.*, **1986**, 1669; b) M. Nakamoto, K. Tanaka, and T. Tanaka, *Bull. Chem. Soc. Jpn.*, **61**, 4099 (1988).
- 35) a) K. Tanaka, T. Tanaka, and I. Kawafune, *Inorg. Chem.*, **23**, 517 (1984); b) K. Tanaka, M. Moriya, and T. Tanaka, *Inorg. Chem.*, **25**, 835 (1986); c) M. Masanaga, S. Kuwabata, K. Tanaka, and T. Tanaka, *Chem. Lett.*, **1986**, 1531.